

CRSM: Crowdsourcing based Road Surface Monitoring

Kongyang Chen^{1,2}, Mingming Lu³, Guang Tan¹, and Jie Wu⁴

¹SIAT, Chinese Academy of Sciences, Shenzhen 518055, China

²University of Chinese Academy of Sciences, Beijing 100049, China

³Central South University, Changsha 410083, China

⁴Temple University, PA 19122

Email: {ky.chen, guang.tan}@siat.ac.cn, ming.lu@gmail.com, jiewu@temple.edu

Abstract—Detecting road potholes and road roughness levels is key to road condition monitoring, which impacts transport safety and driving comfort. We propose a crowdsourcing based road surface monitoring system, simply called *CRSM*. *CRSM* can effectively detect road potholes and evaluate road roughness levels using our hardware modules mounted on distributed vehicles. These modules use low-end accelerometers and GPS devices to obtain vibration pattern, location, and vehicle velocity. Considering the high cost of onboard storage and wireless transmission, a novel light-weight data mining algorithm is proposed to detect road surface events and transmit potential pothole information to a central server. The server gathers reports from the multiple vehicles, and makes a comprehensive evaluation on road surface quality. We have implemented a product-quality system and deployed it on 100 taxis in the Shenzhen urban area. The results show that *CRSM* can detect road potholes with up to 90% accuracy, and nearly zero false alarms. *CRSM* can also evaluate road roughness levels correctly, even with some interferences from small bumps or potholes.

Keywords—Road surface monitoring, Pothole detection, Gaussian Mixture Model, Road surface roughness.

I. INTRODUCTION

Road surface conditions have been a public concern in our society. City municipalities have paid millions of dollars to detect, maintain, and repair the roadways each year. A study by the U.S. department of transportation has shown that road condition is an essential factor of highway quality [1]. One of the main road surface condition metrics is the density of road potholes, which can cause serious damage, and should be repaired as early as possible. In addition, the roughness level of road surfaces is also an important metric that reflects the condition of road health. This paper seeks to evaluate these two metrics in an efficient way, following a crowdsourcing approach.

Our basic observation is that accelerometers will experience significant vibration when the vehicle is passing an "abnormal" section of road (e.g., potholes, manholes, and expansion joints), thus producing abnormal readings compared with data from smooth road surfaces. We only store and transmit data associated with these abnormal events to a central server. Meanwhile, we try to establish a relationship between the road surface roughness level and acceleration

signal. According to the Technical Code of Maintenance for Urban Road CJJ36-2006 [13], one of the industry standards in China, we provide a low-cost solution for road roughness detection.

We describe the design and implementation of a crowdsourcing based road surface monitoring system, simply called *CRSM*. It can detect road potholes and evaluate road roughness levels with our hardware modules installed on distributed vehicles, which are wirelessly connected to a central server. A *CRSM* module consists of an accelerometer and a GPS module to identify road vibration and obtain location and vehicle velocity. To minimize storage and transmission costs, a light-weight data mining algorithm, namely *i-GMM* (improved Gaussian Mixture Model), is proposed to detect road surface events, and transmit pothole information to the server. *CRSM* also presents a road roughness classification algorithm to determine the road roughness level. Experimental results show that *CRSM* can detect road potholes with up to 90% accuracy, with nearly zero false alarms. *CRSM* can also evaluate road roughness levels correctly, even with some interferences from small bumps or potholes.

In summary, we make the following contributions:

- We design and implement a crowdsourcing-based road surface monitoring system for both pothole detection and road surface roughness evaluation.
- We propose a mining algorithm for event detection. We analyze two drawbacks of the traditional Gaussian Mixture Model (GMM), and propose an improved version to compensate for the different vibration patterns with different velocities.
- We present an online algorithm for road surface roughness evaluation in compliance with industry standards.
- We show the evaluation results from a product system deployed on 100 taxis in the Shenzhen urban region.

The remainder of this paper is organized as follows. Section II provides a brief overview of previous works. Section III gives an overview of our system architecture. Section IV and Section V discuss the road pothole detection and road roughness level classification, respectively. Section VI presents

our actual evaluation on real taxis. Finally, Section VII concludes this paper.

II. RELATED WORK

A. Road pothole detection

Many road pothole detection solutions have been proposed in the literature. In [2], citizens are encouraged to share and upload the pothole information to public online websites. Various sensors such as 3D laser scanning devices, along with 3D reconstruction algorithms, are used to measure the size of road potholes [3], [4], [5]. In [6], [7], cameras are installed on vehicles to record road videos, from which road condition is inferred. These pothole detection techniques are not convenient enough for deployment, or too expensive for wide adoption.

Recently, accelerometers have been increasingly utilized in road condition monitoring. Intuitively, a vehicle vibrates more significantly than normal when passing potholes, contraction joints, manholes, expansion joints, etc. The vibration can be effectively captured by an onboard accelerometer. Given an accelerometer and a GPS device, we can identify a road vibration situation and its corresponding location [8]. This method needs to sense, store, and upload all the acceleration and GPS data to a central server for further processing [9], [10], [11]. However, the high demand for data storage and data transmission remains a challenging issue.

B. Road roughness level classification

City municipalities are very concerned with road surface roughness information, and the whole road will be repaired when it is considered to be unqualified. Xu et al. [14] present a criterion of road roughness based on power spectral density of vehicle vibration. Semiha et al. [15] study the random vibration characteristics of the quarter car model to describe the vehicle vibration. Zhang et al. [16] discuss a roughness measurement system based on the laser range finder. Dyer et al. [17] describe how to estimate international roughness index from noisy profilograph measurements. Hostettler et al. [12] summarize current equipments for road condition measurement, composed of accelerometers, distance instruments, graphic displays, or some other instruments. These road condition evaluation systems are highly expensive, costing 8,000 to 220,000 dollars for a single vehicle.

III. SYSTEM OVERVIEW

CRSM uses a set of hardware devices installed on vehicles for data collection and a central server for multi-source data fusion. The system architecture is illustrated in Figure 1.

Each onboard hardware device is composed of a micro-controller (MCU), a GPS module, a three-axis accelerometer, and a GSM module. When the vehicle is traveling, the accelerometer reads continuous acceleration data; the GPS module outputs accurate time, location, and velocity of the vehicle; the MCU executes algorithms to extract useful data, and the GSM module transmits the results to the central server.

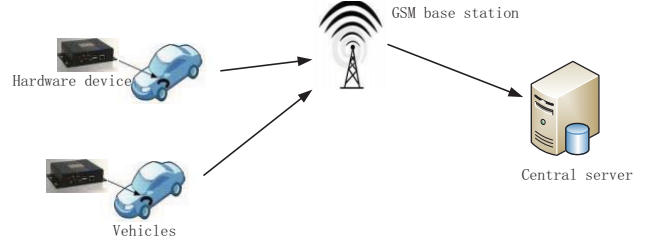


Fig. 1: CRSM system architecture.

The GSM traffic presents a major cost in the system. In our system, for example, the GSM data budget is no more than 30 mega bytes per month. We therefore cannot transmit the raw data to the central server, as the data is too large in size. Because of this, we transmit only useful information, which is determined by a light weight online data mining algorithm.

IV. ROAD POTHOLE DETECTION

The CRSM system selectively reports useful data to the central server by discarding acceleration data on smooth roads. First, we design an event detection algorithm to identify “abnormal” vibrations. Then the central server will further analyze the data from multiple vehicles to obtain more accurate results.

A. The improved GMM (i-GMM) algorithm

Event detection is a process for identifying potential potholes on the road surface [18]. An onboard accelerometer can sense the vehicle vibration by examining the z-axis acceleration. Normally, the vibration on abnormal road sections is greater than that on smooth sections, so an abrupt increase of z-axis acceleration often signify a pothole.

The Z-peak method declares an event if the current z-axis acceleration is larger than a predefined threshold. However, the vehicle vibration and acceleration vary greatly on different roads, or even different driving velocities. It is therefore impossible to determine a universal threshold that applies to all possible situations.

To address this problem, we introduce a Gaussian Mixture Model (GMM) algorithm for event detection. The GMM can learn the background signal online, without the need to train parameters for different road conditions beforehand, which has great distinction with previous methods. Furthermore, we propose an i-GMM algorithm to overcome the drawbacks of GMM.

B. The Gaussian Mixture Model (GMM)

The z-axis acceleration signal captured from a smooth road can be fitted by a Gaussian distribution. An example of empirical z-axis acceleration is shown in Figure 2, which confirms this hypothesis. The Gaussian distribution with mean μ and variance σ^2 :

$$\eta(x|\mu, \sigma^2) = \frac{1}{\sqrt{2\pi}\sigma} e^{-(x-\mu)^2/2\sigma^2} \quad (1)$$

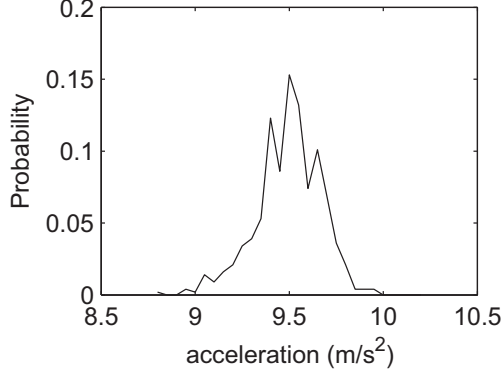


Fig. 2: Distribution of the z-axis acceleration from a smooth road.

can be dynamically updated from historic information. In our situation, the magnitude of vibration caused by a pothole is much greater than that caused by a smooth road surface. So a signal X is considered as a pothole if it deviates widely from the mean μ of the smooth road. That is to say, X is a pothole signal if the absolute difference of X and μ is greater than a predefined threshold M_{th} times the standard variance σ , that is

$$\left| \frac{X - \mu}{\sigma} \right| > M_{th} \quad (2)$$

Otherwise, X is considered to be a smooth road signal, and its mean μ and variance σ will be modified as follows:

$$\begin{aligned} \mu' &= (1 - \delta)\mu + \delta X \\ \sigma'^2 &= (1 - \delta)\sigma^2 + \delta(X - \mu)^2 \\ \delta &= \alpha\eta(X|\mu, \sigma^2) \end{aligned} \quad (3)$$

where α is a learning rate, and δ is α time probability density function learnt from the past signals.

The above method is the single Gaussian model, which is only a rough approximation of the background signal. A better solution with more accuracy is given by the Gaussian Mixture Model (GMM), which uses K Gaussian distributions to capture the background signals [18], [19], as is evident from the multiple peaks in Figure 2. An intuitive idea is that acceleration signals are developed by various sources and errors which follow their respective Gaussian distributions. So the GMM assigns a weight ω_k to each of the K Gaussian distributions $\omega_k\eta(\mu_k, \sigma_k^2, \omega_k)$ following $\sum_{k=1}^K \omega_k = 1$.

Consider a newly sampled signal X . The GMM first updates the parameters of each Gaussian distribution to best fit X , and then estimates X as a background or an event.

1) *Online update*: If the signal X matches any of the K Gaussian distributions, it means that the current GMM is robust for X . Suppose $\eta(\mu_k, \sigma_k^2, \omega_k)$ is a matched distribution. We

add its weight and update its mean and variance as follows

$$\begin{aligned} \mu'_k &= (1 - \delta)\mu_k + \delta X \\ \sigma_k'^2 &= (1 - \delta)\sigma_k^2 + \delta(X - \mu_k)^2 \\ \omega'_k &= (1 - \alpha)\omega_k + \alpha \\ \delta &= \alpha\eta(\mu_k, \sigma_k^2, \omega_k) \end{aligned} \quad (4)$$

where α is a learning rate.

In this case, an unmatched distribution holds the same mean and variance, but its weight should be decreased. Its parameters are updated as follows

$$\begin{aligned} \mu'_k &= \mu_k \\ \sigma_k'^2 &= \sigma_k^2 \\ \omega'_k &= (1 - \alpha)\omega_k \end{aligned} \quad (5)$$

If the signal X does not match any of the K Gaussian distributions, it means that the current GMM is not robust for X . The least probable distribution with the lowest ω_k is replaced with a new distribution to better fit the current signal X . This new distribution takes on the current signal X as its mean value, with a predefined high variance and a low weight.

$$\begin{aligned} k &= \underset{k}{\operatorname{argmin}} \omega_k \\ \mu'_k &= X \\ \sigma_k'^2 &= \sigma_0^2 \\ \omega'_k &= \omega_0 \end{aligned} \quad (6)$$

where weights are normalized so that $\sum_{k=1}^K \omega'_k = 1$;

2) *Background model estimation*: After online update, we would like to determine whether the current signal X is an event. Among the K Gaussian distributions, we are interested in distributions which are most likely to be produced by the background. Intuitively, these distributions have the highest weights and lowest variances. At the same time, the least likely distributions are likely modeled as old historical signals or updated distributions with a predefined value, whose effect we will downplay.

Next, the K Gaussian distributions are sorted with the value of $\omega'_k/\sigma_k'^2$ to place the most likely distributions in a list. Then, the B most likely distributions are selected as the background model,

$$B = \underset{b}{\operatorname{argmin}} \left(\sum_{k=1}^b \omega'_k > T \right) \quad (7)$$

where T is a predefined threshold to determine how many distributions are used to represent the current background.

Finally, the current signal x is estimated with the B selected distributions. Similar to the single Gaussian model, X is considered as an event if all these B distributions $\eta(\mu'_k, \sigma_k'^2, \omega'_k)$ satisfy

$$M_k = \left| \frac{X - \mu'_k}{\sigma_k'} \right| > M_{th} \quad (8)$$

where M_{th} is a predefined event detection threshold. Otherwise, X is not considered as an event.

C. Two drawbacks of the GMM

When we used the GMM for event detection, we found two drawbacks caused by the variation in velocity.

1) *Drawback 1: fixed event detection threshold:* Obviously, vehicle vibration is highly affected by driving velocity. For example, when driving at a high velocity, the vehicle vibrates greatly and our onboard accelerometer will generate higher vibration amplitude. In fact, Watts et al. [20] have carried out some experiments on ground vibration levels with different vehicle velocities, and pointed out that vehicle vibration levels and driving velocities are roughly in linear relationship when velocities are in the range from 15km/h to 45km/h. So, we can view z-axis accelerations as roughly proportional to vehicle velocity.

Suppose an experimental vehicle moves at a high velocity on a smooth road, causing z-axis acceleration to vary greatly. When applying the GMM on this smooth road, unmatched distributions keep their means and variances, and matched distributions update their means and variance as follows:

$$\begin{aligned}\mu'_k &= (1 - \delta)\mu_k + \delta X \\ \sigma'^2_k &= (1 - \delta)\sigma_k^2 + \delta(X - \mu_k)^2 \\ \delta &= \alpha\eta(\mu_k, \sigma_k^2, \omega_k)\end{aligned}\quad (9)$$

where α is a learning rate.

In our experimental scenario, accelerometers have a 100 Hz sampling rate, so even a short segment of road will generate highly redundant raw data. In this case, we should not set the learning rate α too high, otherwise the GMM keeps little historic information and becomes very unstable. Generally, we initialize the learning rate α to 0.03. Obviously, the probability density function $\eta(\mu_k, \sigma_k^2, \omega_k)$ is less than 1, and we have $\delta < \alpha$ and $1 - \delta \gg \delta$.

When the vehicle is traveling on a smooth road, the k^{th} mean of Gaussian distribution μ_k are at the same order of magnitude of the current signal X . Hence, we can deduce that $(1 - \delta)\mu_k \gg \delta X$ and $\mu'_k \approx (1 - \delta)\mu_k$. In other words, the matched distributions decrease their means with a small slope $1 - \delta$. For simplicity, we may consider their means as a constant C_1 in a short time interval. Similarly, we can conclude that the matched distributions decrease their variance with a small slope $1 - \delta$, and can be approximated with a constant C_2 in a short time interval.

Therefore, the event detection expression M_k is as follows:

$$M_k = \left| \frac{X - \mu'_k}{\sigma'_k} \right| \approx \left| \frac{X - C_1}{C_2} \right| \quad (10)$$

Clearly, M_k is roughly linear with the acceleration signal X , and then approximately proportional to vehicle velocity V , too.

Suppose the vehicle is traveling at a high velocity, then the GMM event detection expression M_k becomes larger. This causes false alarms when M_k is greater than the fixed threshold M_{th} . Figure 3 shows the z-axis acceleration and event detection expression on a smooth road surface. We see that the GMM event detection expression (Figure 3(b) real line)

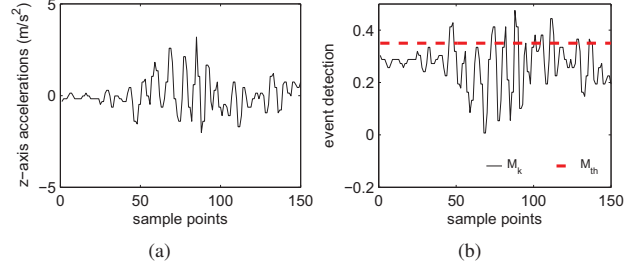


Fig. 3: Event detection at high velocity, (a) z-axis acceleration, (b) event detection with false alarms.

is very similar to the z-axis acceleration (Figure 3(a)). We also observe that the event detection expression M_k is sometimes greater than the predefined threshold M_{th} (Figure 3(b) red dashed line), which causes false alarms.

For similar reasons, a low traveling velocity leads to event missings when a fixed event detection threshold is applied.

2) *Drawback 2: fixed learning rate:* The GMM uses a fixed learning rate α to update the mean, variance, and weight of each Gaussian distribution, as if the current signal and historic information were equally important. However, this rule no longer applies when the vehicle velocity changes. For instance, when the vehicle's velocity increases greatly, the z-axis acceleration will also increase greatly, which results in a relatively large distance to historic information. With fixed learning rate, it will take a long time to learn and build accurate Gaussian distributions [21].

To deal with this problem, we need to increase the GMM learning rate and bias the learning process toward the current signal. Similarly, we should increase the learning rate when the velocity decreases greatly, while use a small learning rate when the vehicle velocity is almost the same.

In summary, we can conclude that a large learning rate is suitable for a big velocity changes, and a small learning rate for small velocity changes.

D. i-GMM

To overcome these above two drawbacks of the GMM, we propose a novel i-GMM algorithm to accommodate to the variability of velocity.

1) *Event detection threshold:* With a fixed event detection threshold, a high velocity will produce more false alarms, and a low velocity will increase missed events. For this reason, the event detection threshold is changed to a parameter which is roughly linear with the current velocity. The above event detection rule is modified as follows:

The current signal X is considered as an event only if all the B distributions $\eta(\mu'_k, \sigma'^2_k, \omega'_k)$ satisfy

$$M_k = \left| \frac{X - \mu'_k}{\sigma'_k} \right| > M_{th} \frac{V}{V_{th}} \quad (11)$$

where V is the current velocity, and V_{th} is a velocity threshold.

2) *Learning rate update*: Based on the above discussion, the learning rate is related to the change of velocity. A high learning rate is used for big velocity changes, and a small learning rate for small velocity changes.

It is found empirically that the learning rate at the moment t can be adjusted as follows:

$$\alpha_t = \alpha_{min} + (\alpha_{max} - \alpha_{min}) \cdot (1 - e^{-(\Delta V_t/V_0)^2}) \quad (12)$$

$$\Delta V_t = V_t - V_{t-1}$$

where α_{min} and α_{max} are the minimum and maximum learning rates; ΔV_t is the velocity change at time t ; V_0 is a velocity threshold; V_t and V_{t-1} are velocities at t and $t-1$ moments, respectively.

E. Pothole filters and data fusion

The CRSM system uses an i-GMM for event detection. Our central server will gather, clean, and fuse event data from these multiple vehicles.

1) *Pothole filters*: We apply four pothole filters to remove anomalous events, similar to Pothole Patrol [9]:

- **Velocity filter**: it removes events with zero velocity or very low velocity, such as opening or closing the vehicle panels. It rejects events whose velocity is lower than a threshold T_V .
- **Z-axis acceleration filter**: it takes out events with low z-axis acceleration peaks like small bumps. It refuses events whose z-axis acceleration is lower than a threshold T_Z .
- **X-z acceleration ratio filter**: it deletes events with a small ratio of x-axis acceleration to z-axis acceleration, such as expansion joints and contraction joints. It discards events whose x-z acceleration ratio is lower than a threshold T_{XZ} .
- **Velocity vs. z-axis acceleration ratio filters**: it removes events with a high ratio of velocity to z-axis acceleration, mainly caused by high velocity vibration. It rejects events whose velocity vs. z acceleration ratio is higher than a threshold T_{VZ} .

2) *Data fusion*: After pothole filtering, the central server gathers multiple vehicles' pothole detection results. Next, it counts report times of each potential potholes. Finally, it declares a pothole where report times are larger than a threshold P ; otherwise it marks these pothole detection results as false alarms.

V. ROAD SURFACE ROUGHNESS CLASSIFICATION

We propose an online data mining algorithm to classify road surface roughness into four levels.

A. Distributed road roughness classification

1) *International roughness index*: International Roughness Index (IRI) is the most widely used metric to evaluate road roughness in highway transportation. It reflects the global vibration of the road, which can be measured by an accelerometer.

Lou et al. [22] show that the empirical relationship between IRI and standard deviation of vibration σ approximates to the following regression equation:

$$IRI = \frac{\sigma - 0.013}{0.5926} \quad (13)$$

2) *Road roughness level classification*: Technical Code of Maintenance for Urban Road CJJ36-2006 [13] is an industry standard in China. This industry standard indicates that road roughness levels can be evaluated by a comprehensive driving comfortable metric, namely Riding Quality Index (RQI).

Generally, road roughness is classified into four levels, including excellent, good, qualified, and unqualified, with different RQIs and driving velocities. These evaluation standards for pavement roughness are listed in Table I.

Yang [13] shows that the relationship between RQI and IRI can be described mathematically as follows:

$$RQI = 4.98 - 0.34 \cdot IRI \quad (14)$$

Additionally, the numerical value of RQIs varies from 0 to 5 normally. We set RQI to 0 when it is negative.

In the CRSM system, the onboard hardware devices collect accelerations, calculate the standard deviation σ and IRI, classify road roughness into these above four levels, and transmit recent road roughness levels to the central server periodically.

B. Central server data fusion

The central server collects reports from these distributed CRSM hardware devices, and then makes a comprehensive evaluation of these road roughness levels of different road sections in a city region.

VI. EVALUATION

This section presents the evaluation of the CRSM system.

A. Experimental setting

We conducted experiments with a total of 100 vehicles in the Shenzhen urban region. Each vehicle is equipped with a CRSM device, and can generate GPS and acceleration readings. To get ground truth for our experiments, we employed another vehicle with a CRSM device and a camera to record road surface videos for comparison.

The CRSM module is installed at the same location of each vehicle. In our context, it is attached to the right side of the dashboard to sense the vibration effectively, while the GPS receiver is fixed on the right front of the vehicle for better signal intensity. The three-axis accelerometer is installed inside

TABLE I: EVALUATION STANDARDS FOR ROAD ROUGHNESS LEVELS.

$v(\text{km/h})$	RQI	Pavement roughness level
$v > 80$	$\text{RQI} > 3.6$	excellent
	$3.0 < \text{RQI} < 3.6$	good
	$2.5 < \text{RQI} < 3.0$	qualified
	$0 < \text{RQI} < 2.5$	unqualified
$40 < v < 80$	$\text{RQI} > 3.2$	excellent
	$2.8 < \text{RQI} < 3.2$	good
	$2.4 < \text{RQI} < 2.8$	qualified
	$0 < \text{RQI} < 2.4$	unqualified
$v < 40$	$\text{RQI} > 3.0$	excellent
	$2.6 < \text{RQI} < 3.0$	good
	$2.2 < \text{RQI} < 2.6$	qualified
	$0 < \text{RQI} < 2.2$	unqualified

the hardware device. However, we need to place the three-axis accelerometer in a specified direction, where its x-axis is kept with the same direction with the driving direction, y-axis in the corresponding horizontal direction, and the z-axis in the vertical direction.

B. Raw data cleaning

As mentioned above, CRSM onboard module monitors road condition with a three-axis accelerometer and a GPS device. Here, the three-axis accelerometer periodically generates 100 data samples every second. Meanwhile, the GPS device provides one data sample, including current time, location and driving velocity.

In practical environments, we face several technical challenges. First, the GPS receiver often falls to work in urban canyons with tall buildings and tunnels, which lead to many GPS data missing. Second, Our GPS receiver need very long time to get a fix position after power on, and some GPS receivers provide wrong position in the first few seconds. Third, we might miss raw data or get wrong raw data owing to transmission errors, especially when the network is busy.

To overcome these three problems, we propose an effective data cleaning algorithm. We first sort the raw data in time sequence, detect GPS bad zones with very long data missing or discontinuity, and remove these bad zones directly. Then, we check up on transmission errors and short GPS missings, and record the time index. Next, we generates interpolated points in curves to get continuous data. Finally, Our data cleaning algorithm results are organized in four elements as follows: $\langle \text{time, location, velocity, three-axis acceleration} \rangle$.

C. Road pothole detection

The CRSM modules apply the i-GMM for event detection, and transmit useful data to the central server.

1) *Event detection*: There are several thresholds to be determined in the i-GMM. As we cannot reduce the false alarm and the missing rate at the same time, there is always a tradeoff between them. In CRSM, we would like to keep more potential

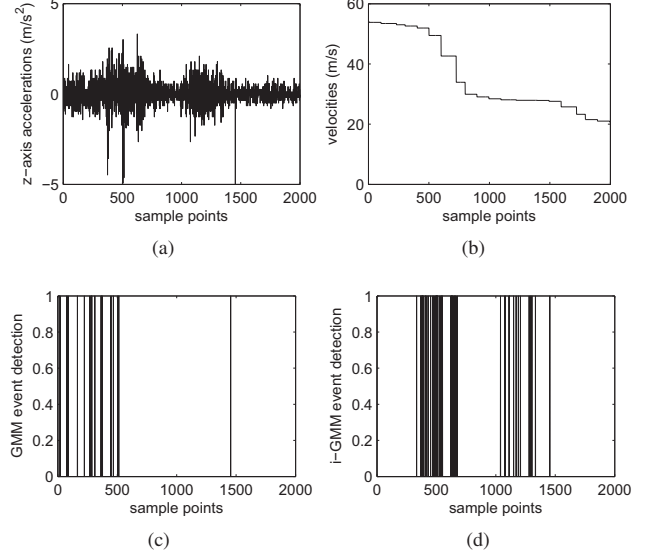


Fig. 4: Comparison of the GMM event detection and the i-GMM event detection, (a) z-axis acceleration, (b) velocity, (c) the GMM event detection, (d) the i-GMM event detection.

potholes, even with some false alarms. Actually, most false alarms can be removed by pothole filters and data fusion in the central server. Generally, we keep the missed event rate less than 5% with all thresholds as following:

Gaussian number $K = 4$, initial Gaussian mean $\mu_0 = 0$, variance $\sigma_0 = 10$, weight $\omega_0 = 0.15$, sum of most likely distribution weight $T = 0.7$, maximum and minimum of learning rate $\alpha_{min} = 0.02$, $\alpha_{max} = 0.04$, event detection threshold $M_{th} = 0.25$, and velocity threshold $V_{th} = 50$.

Figure 4 shows the comparison of the GMM event detection and the i-GMM event detection. Figure 4(a) and 4(b) are the z-axis acceleration and velocity, respectively, Figure 4(c) and 4(d) are the event detection results of the GMM and the i-GMM, where each vertical line indicates an effect event. We can infer that the GMM has many false alarms at a large velocity, with missing events at a small velocity, while i-GMM can settle this problem.

2) *Pothole detection*: Central server applies four pothole filters to remove disturbance events, and combine multiple vehicles' pothole detection results.

Table II lists pothole events and several disturbance events as well as their occurrence numbers. Four potholes filters are utilized to remove these spurious events later. Figure 5 shows the cumulative density function (CDF) that describes the feature of each filter. Table III lists the pothole recognition accuracy and false alarms of each filter.

Figure 5(a) presents the CDF of velocity filter, which removes events with small velocities. With $T_V = 16$, it rejects all low velocity events with nearly 88% potholes detection accuracy.

TABLE II: REPORTED NUMBERS OF EVENT TYPES.

Event types	Occurrences
Potholes	178
Low speed events	226
Small bumps	51
Expansions	27
High speed events	38

TABLE III: POTHOLES RECOGNITION NUMBER AND POT-HOLE FALSE ALARM NUMBER OF EACH FILTER.

Filters	Accuracy	False alarms
Velocity filter	156	0
Z-acceleration filter	151	13
X-z ratio filter	136	6
Velocity vs. z ratio filter	163	1

Figure 5(b) shows the CDF of z-axis acceleration filter, which discards events with small z-axis accelerations like small bumps. With $T_Z = 1.82$, it achieves 85% pothole detection accuracy with 7.9% of false alarms.

Figure 5(c) describes the CDF of x-z acceleration ratio filter, which refuses events with a small ratio of x-axis acceleration to z-axis acceleration like expansion joints. With $T_{XZ} = 0.06$, it acquires 76% pothole detection accuracy with 4.2% of false alarms.

Figure 5(d) presents the CDF of velocity vs. z-axis acceleration ratio filter, which removes events with high velocity vibration. With $T_{VZ} = 16$, it obtains 92% pothole detection accuracy with 0.6% false alarms only.

With distributed vehicle data fusion, we can further reduce the false alarms which appear rarely in other distributed vehicles. In general, the CRSM system can achieve as much as 90% pothole detection, with nearly zero false alarms.

However, there are still two types of events, manholes and decelerating belts, which cause similar vibrations with potholes. Potholes filters and data fusion cannot effectively distinguish these events. Hence, we discover the geographic locations of manholes and decelerating belts from the urban traffic database, and remove these two types of events with their GPS information.

D. Road roughness level classification

We collect accelerations from actual roads with different characters: (I) smooth roads with rare small particles, (II) general roads with some small particles like sands or small stones, (III) roads with small bumps, (IV) roads with potholes.

Figure 6 shows the continuous z-axis accelerations against sampling points on various road types, where (a) to (d) stand for smooth roads, general roads, roads with bumps, and roads with potholes, respectively.

As illustrated in Figure 6(a), the z-axis accelerations on smooth roads are very regular with only small fluctuations

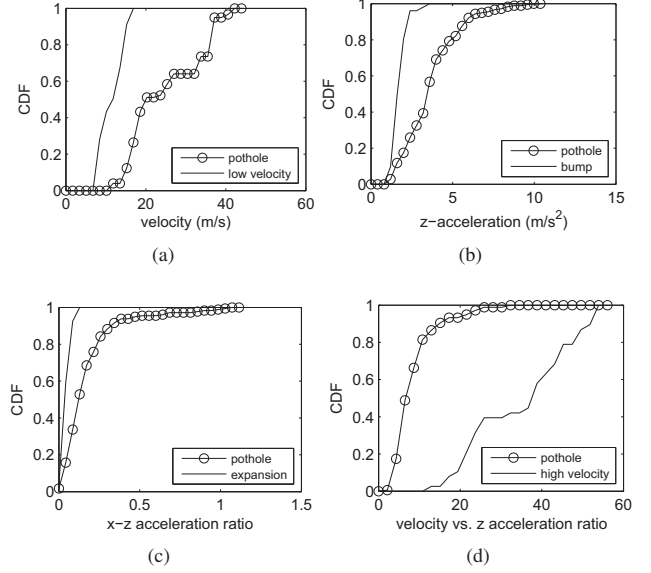


Fig. 5: Four pothole filters, (a) velocity filter, (b) z acceleration filter, (c) x-z acceleration ratio filter, (d) velocity vs. z-axis acceleration ratio filter.

in the middle. From Figure 6(b), we can see that there are relatively larger amplitude in the z-axis accelerations on general roads than on smooth roads. It might be caused by continuous small obstacles or other particles on the road surface, and the overall road condition is very good. Figure 6(c) indicates the z-accelerations on roads with bumps. We find some larger fluctuations due to several small bumps. This road is also considered to be qualified in spite of these disturbances. Figure 6(d) shows the z-axis accelerations data on roads with potholes. The acceleration data are with great fluctuations, and we deduce that the vehicles vibrated strongly when passing by these potholes. The road condition is unqualified in general.

Distributed onboard modules transmit road roughness levels to the central sever periodically. Then road roughness is evaluated into levels with maximum report times in our central server. Road roughness levels of various road types are listed in Table IV. These four road types with different velocities are classified into excellent, good, qualified, unqualified level, which are in conformity with above discussions.

Experimental results show that the CRSM can evaluate road roughness levels correctly, even with some interferences like small bumps or potholes. Furthermore, CRSM onboard module consumes no more than 50 dollars in total, which is only 1/4400 to 1/160 of these existing systems [12] with a cost of about 8,000 to 222,000 dollars. Therefore, CRSM is more likely to be widely adopted in municipal engineering.

VII. CONCLUSION

In this paper, we describe the design and implementation of CRSM, a crowdsourcing-based road surface monitoring system. It can monitor road potholes and road roughness levels

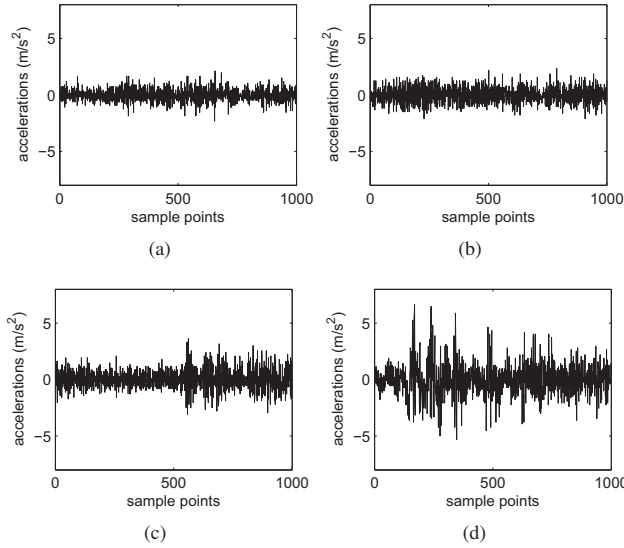


Fig. 6: Continuous z-axis accelerations, (a) smooth roads, (b) general roads, (c) roads with bumps, (d) roads with potholes.

TABLE IV: ROAD ROUGHNESS LEVELS OF VARIOUS ROAD TYPES.

Road type	Velocity	RQI	Road roughness level
Smooth	37.15	3.52	excellent
General	63.86	3.12	good
Bumps	62.36	2.66	qualified
Potholes	37.50	1.14	unqualified

simultaneously with distributed modules mounted on vehicles. Experimental results show that CRSM can detect road potholes with up to 90% accuracy, and nearly zero false alarms. CRSM can also evaluate road roughness levels correctly, even with some interferences from small bumps or potholes.

ACKNOWLEDGMENT

Guang Tan's work was supported by the National Science Foundation of China (NSFC) under Grant 61103243, Youth Innovation Promotion Association, Chinese Academy of Sciences, the Ministry of Science and Technology 863 Key Project No. 2011AA010500, and Shenzhen Overseas High-level Talents Innovation and Entrepreneurship Funds KQC201109050097A. Mingming Lu's work was supported in part by the NSFC under grant 60903222.

REFERENCES

- [1] U.S. Federal Highway Administration. *2010 status of the nation's highways, bridges, and transit: conditions & performance*. <http://www.fhwa.dot.gov/policy/2010cpr/index.htm>.
- [2] ABC7Chicago.com. *Operation Pothole*. <http://abclocal.go.com/wls/feature?section=resources/traffic&id=5791474>.
- [3] Jason M, Claire S, Stephen M, Denis T. *3D laser imaging for surface roughness analysis*. International Journal of Rock Mechanics and Mining Sciences, 2012, 58, 111-117.

- [4] Li Q, Yao M, Yao X, Xu B. *A real-time 3D scanning system for pavement distortion inspection*. Measurement Science and Technology, 2010, 21(1), 15702-15709.
- [5] Hou Z, Wang K, Gong W. *Experimentation of 3D pavement imaging through stereovision*. In: Proceedings of International Conference on Transportation Engineering, 2007, 376-381.
- [6] Yu X, Salari E. *Pavement pothole detection and severity measurement using laser imaging*. In: Proceedings of 2011 IEEE International Conference on Electro/Information Technology, 2011, 1-5.
- [7] Christian K, Ioannis B. *Pothole detection in asphalt pavement images*. Advanced Engineering Informatics, 2011, 25, 507-515.
- [8] Yu, B, Yu X. *Vibration-based system for pavement condition evaluation*. In: Proceedings of the 9th International Conference on Applications of Advanced Technology in Transportation, 2006, 183-189.
- [9] Eriksson J, Girod L, Hull B. *The Pothole Patrol: using a mobile sensor network for road surface monitoring*. In: Proceedings of 6th International Conference on Mobile Systems, Applications, and Services (MobiSys 2008), 2008, 29-39.
- [10] Kasun Z, Chamath K, Gihan S, Shihan W. *A public transport system based sensor network for road surface condition monitoring*. In: Proceedings of the 2007 workshop on Networked systems for developing regions, 2007.
- [11] Prashanth M, Venkata N, Ramachandran R. *Nericell: Rich monitoring of road and traffic conditions using mobile smartphones*. In: Proceedings of 6th International Conference on Embedded Networked Sensor Systems (Sensys 2008), 2008, 323-336.
- [12] Budras J. *A synopsis on the current equipment used for measuring pavement smoothness*. <http://www.fhwa.dot.gov/pavement/smoothness/rough.cfm>.
- [13] Yang S. *Technical Code of Maintenance for Urban Road CJJ36-2006*: China Architecture & Building Press, 2006.
- [14] Xu D, Mohamed A, Yong R, Caporuscio F. *Development of a criterion for road surface roughness based on power spectral density function*. Journal of Terramechanics. 1992, 29, 477-486.
- [15] Semiha T, Huseyin A. *A study of random vibration characteristics of the quarter-car model*. Journal of Sound and Vibration. 2005, 282, 111-124.
- [16] Zhang Y, Ma R. *A study of pavement roughness measurement system based on laser ranger finder*. In: Proceedings of International Conference on Image Analysis and Signal Processing, 2009, 295-299.
- [17] Dyer J, Dyer D, Devore J. *Estimating International Roughness Index from noisy profilograph measurements*. In: Proceedings of IEEE Instrumentation and Measurement Technology Conference, 2009, 1116-1120.
- [18] Tan G, Lu M, Jiang F, Chen K, Huang X, Wu J. *Bumping: A Bump-Aided Inertial Navigation Method for Indoor Vehicles Using Smartphones*. IEEE Transactions on Parallel and Distributed Systems, 2013.
- [19] Lin H, Chuang J, Liu T. *Regularized Background Adaptation: A Novel Learning Rate Control Scheme for Gaussian Mixture Modeling*. IEEE Transactions on Image Processing, 2011, 20, 822-836.
- [20] Mohammad M, Marwan S, Isam S. *Numerical modeling of traffic-induced ground vibration*. Computers and Geotechnics, 2012, 116-123.
- [21] Basharat A, Gritai A, Shah M. *Learning object motion patterns for anomaly detection and improved object detection*. In: Proceedings of 2008 IEEE Conference on Computer Vision and Pattern Recognition (CVPR 2008), 2008, 1-8.
- [22] Lou S, Wang Y, Xu C. *Study of calculation of IRI based on power spectral density of pavement surface roughness*. Journal of Highway and Transportation Research and Development, 2007, 24, 12-15.